CILAMCE2014
XXXV IBERIAN LATIN AMERICAN CONGRESS ON COMPUTATIONAL METHODS IN ENGINEERING
FORTALEZA - CEARÁ - BRAZIL | NOVEMBER 23-26, 2014

A STRESS TRANSFER FUNCTION METHODOLOGY FOR FLEXIBLE RISER TENSILE ARMORS

Joakim A Taby

joakim.marintek@sintef.no

MARINTEK/Instituto SINTEF do Brasil (ISdB)

Rua Bambina 126, 22251-050 Rio de Janeiro, RJ, Brazil

Philippe Mainçon

Philippe.Maincon@sintef.no

MARINTEK, currently SINTEF Materials & Chemistry

P:O: Box 4760 Sluppen NO-7465 Trondheim, Norway

Marcelo Caire

marcelo.caire@sintefbrasil.org.br

Instituto SINTEF do Brasil (ISdB)

Rua Bambina 126, 22251-050 Rio de Janeiro, RJ, Brazil

Abstract. *Flexible risers are widely used in the offshore industry to transport liquids and gas between the seabed and platforms. They are currently being put to use in ever more demanding environments in terms of water depths, temperature, pressure and corrosive fluids and consequently an accurate fatigue assessment is required to keep the level of analysis uncertainties low. A detailed finite element model of the flexible riser cross section is used to calibrate a stress transfer function, allowing the fast determination of stresses in the tensile armors from timeseries of tension and curvatures. This reduces the number of local analyses, accounts for load directions, and allows handling load combinations (low frequency vessel motions, wave response, VIV). The resulting stress time series can then be directly processed with a rainflow counting technique to evaluate the fatigue damage at several points in the cross section using an SN curve and Miner-Palmgreen summation. In the present paper the method is outlined and a comparison with direct calculation on the local model is presented.*

Keywords: *Flexible risers, tensile armor, stress transfer function*

1 INTRODUCTION

The structural response of flexible risers is highly nonlinear. The geometry of the pressure armor, and the contact forces and friction between adjacent components within the riser are important sources of non-linearity. The geometry of the pressure armor gives low stiffness in bending until a limiting curvature is reached and the geometry locks. This is however a state that is not permitted. Design codes such as API 17J (API, 2009) state that the minimum bending radius should be at least 1.1 times the radius that causes locking. Hence locking, adressed in extreme curvature analysis, is not a concern in fatigue analysis. Frictional forces however are a source of non-linearity that is present also in normal operations, and should thus be accounted for. To account for this nonlinearity, and to calculate stresses arising in the cross section from a given deformation, tailor made software are usually applied. Even though these software utilize assumptions that make the solution faster than what general solvers would have achieved, the local analyses are still quite computationally costly. In this paper we will present a method to use a set of short local analyses in order to extract results to calibrate a stress transfer function for the tensile armor wires, which takes care of the nonlinearity described above. This implementation of the method is to a large degree based upon the work of Doynov et. al (2007), and was carried out at MARINTEK. The method will be described in the following section, while a case study is presented in section 3. The results of the case study are discussed in section 4 and finally conclusions are given in 5.

2 METHODOLOGY

The stresses in the armor wires can be split into four contributions, as shown in Figure 1. Of these the bending around the weak and strong axis can be taken to be dependent only on the instantaneous curvature of the riser, and the tensile stress can be assumed to be only dependent on the instantaneous wall tension of the riser, pressure assumed constant. The friction stresses however are history dependent quantities. The stress transfer function method needs to keep track of the friction state to estimate these correctly. Here the friction is dependent on the instantaneous tension, and the curvature history, as pressure is taken to remain constant within each time history given.

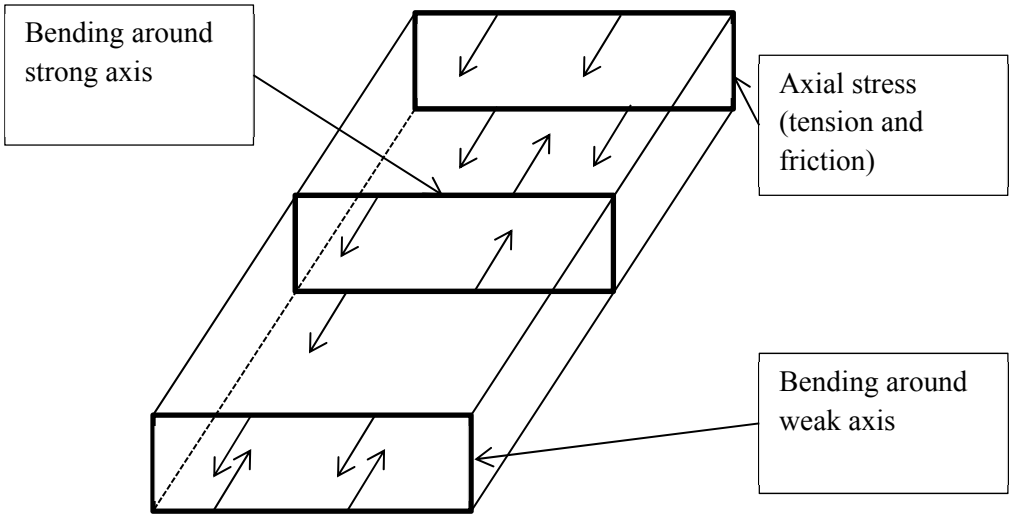

Figure 1: Stress components of tensile armor wire

Local analyses are run to calibrate the stress transfer function algorithm. For a set of different tensions the cross section is pressurized to the given pressure level, tensioned and bent two and a half cycle to a level inducing slipping of both layers. The stresses are calculated using the two coordinate system indicated in Figure 2.

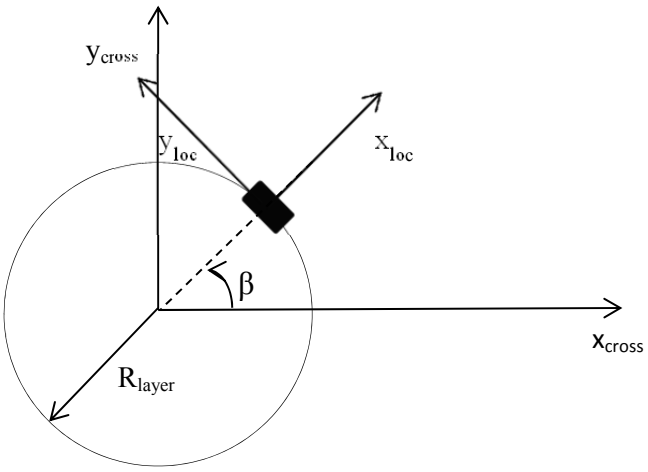

Figure 2: Coordinate systems and definitions.

The axial stress due to tension at every instant can afterwards be found as a lookup of axial stresses due to the different tensions computed in the direct analysis. For the bending stresses an assumption has to be made for the deformation pattern of the tendons due to bending. According to Sævik (1992) the two bounding curves for the deformation pattern are

the geodesic (no transverse friction) and the loxodromic (no transverse displacement) curves. In the same thesis it is also found that the transverse displacement during a dynamic cycle will be small, thus justifying the use of the loxodromic curve for stress calculations. In the current work the loxodromic curve assumption is hence applied. The bending stress around the weak axis of the tendon hence comes out as:

$$\sigma_{b,weak} = E \cdot x_{loc} \,.\cos^4 \alpha \cdot \left(\kappa_y \cdot \cos\beta + \kappa_x \cdot \sin\beta\right) \tag{1}$$

where α is the lay angle of the component in question and κ_x and κ_y are the riser curvatures around the corresponding axes. The bending stress around the strong axis analogously comes out as:

$$\sigma_{b,strong} = E \cdot y_{loc} \cos\alpha \cdot (1 + \sin^2\alpha)\left(-\kappa_y \cdot \sin\beta + \kappa_x \cdot \cos\beta\right) \tag{2}$$

As mentioned, the stress components found so far are taken to be independent of time history. This is not valid for the frictional stresses, which are of course strongly path dependent. The other assumptions used in the stress transfer function are discussed in the following section.

2.1 **Assumptions**

Many of the assumptions applied in the stress transfer function are the same as in the Bflex2010 mode that assumes locally constant curvature and axisymmetric contact pressure (Sævik, 2010). These assumptions are thus only mentioned here since they have been thoroughly discussed elsewhere (Sævik, 2010): the tendons stay on the loxodromic curve, and the axial deformation in the tendon can be neglected when compared to relative sliding.

Two additional assumptions are implied in the stress transfer function. The first one is that each tendon armor layer goes instantaneously from full stick to full slip. The curvature stress relation is hence a bilinear curve for each point in the crossection.

In Bflex2010 on the other hand, the slip is taken to occur gradually over the cross section. The slip onset happens when the shear stresses overcome the available friction at the neutral axis at a curvature found as:

$$\kappa_c = \frac{\mu\left(q_r^i + q_r^{i+1}\right)}{EA\cos^2\alpha \sin\alpha} \tag{3}$$

where μ is the friction factor, $q_r^i + q_r^{i+1}$ are the line loads on the inner and outer side of the tendon, and *EA* is the axial stiffness. The corresponding stress is found as:

$$\sigma(\beta) = \frac{\mu\left(q_r^i + q_r^{i+1}\right)R}{\mathrm{A}\sin\alpha} \tag{4}$$

For full slip the stress can be found from integrating the maximum traction along the wire yielding:

$$\sigma(\beta) = \frac{\pi}{2}\frac{\mu\left(q_r^i + q_r^{i+1}\right)R}{\mathrm{A}\sin\alpha} \tag{5}$$

Between first and full slip the cross section will be partly in slip. As mentioned above, this is not taken into account in the stress transfer function.

The second assumption specific to the stress transfer function is that there exists a riser curvature for which all tendons in the same layer experience no shear stresses in their contact with neighbouring layers. Hence the curvature vector of the shear free configuration suffices to keep track of the tendon state, instead of giving each tendon of interest its own instance of a stick-slip model. Further, this implies that the stress distribution will remain sinusoidal around the layer, also in the slip domain.

With these assumptions in place the frictional stress in each tendon at a time instance can be found as:

$$\sigma_{fric,n+1} = [\cos\beta \quad \sin\beta] \cdot K_{stick} \cdot \left(\boldsymbol{\kappa}_{n+1} - \boldsymbol{\kappa}_{sf,n} - \boldsymbol{\delta\kappa}_{sf}\right) \tag{6}$$

Where σ_{fric} is the friction stress at a given position of the crossection at step *n+1*, K_{stick} is the stick stiffness at the given tension, $\boldsymbol{\kappa}_{n+1}$ is the two dimensional curvature vector at step *n+1*, $\boldsymbol{\kappa}_{sf,n}$ was the stressfree curvature at step *n,* and $\boldsymbol{\delta\kappa}_{sf}$ is the shift in stressfree curvature vector over the last step. The resulting stress-curvature relation from Bflex2010 and the stress transfer function are shown for two different points in the cross section in Figure 3.

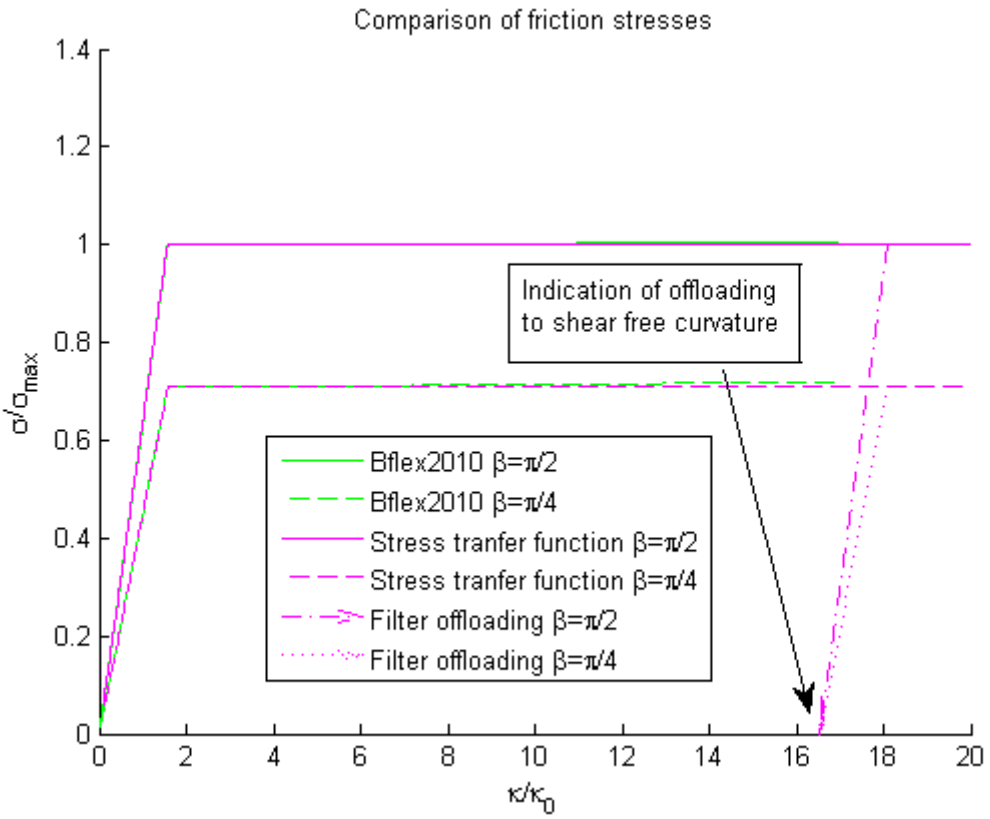

Figure 3: Stress curvature relation from Bflex2010 and stress transfer function.

As can be seen in Figure 3, both Bflex2010 and the stress transfer function gives stresses proportional to the projected curvature at the point where the stress is calculated. The approximation applied in both the stress transfer function and Bflex2010 gives conservative results.

3 CASE STUDY

The case study is based on a local model based on the cross-section presented by Witz (1996). In this publication, we have all data needed to build a local model of a 2.5 inch riser, except the friction factor which was put to 0.16 between all layers. The internal pressure applied in this work is 300 bar in accordance with the high pressure case in Witz (1996).

In the case study, results from a local model were compared with results from the stress transfer function. The inputs were tension and curvature from a global analysis in a related project. The sea state was an *Hs* of 6.3 meters and a *Tp* of 6 seconds, which corresponds to a sea state on the severe side of what normally contributes most to the fatigue damage.

In the direct calculation with the local model the curvatures were put on as rotations in the model ends. As it proved difficult to tune the model to give the exact same curvature

history as the input time history the following procedure were implemented for comparison purposes:

1) Apply the tension and curvature time history on a local model directly
2) Post process the results, including curvature time series
3) Apply the resulting curvature time series on the stress transfer function.

This is obviously not a viable procedure to get the right fatigue estimation from the time series, but as the purpose of this work is to compare the stresses predicted from a local model, with that of the stress transfer function, it was deemed fit for purpose.

The time series of tension and curvature that was used for comparison is shown in Figure 4.

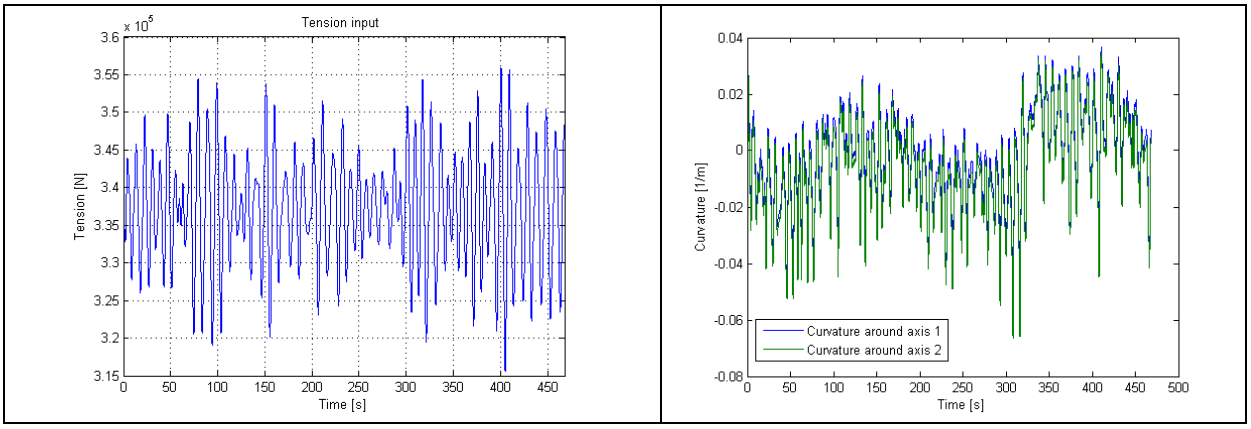

Figure 4: Input time series of tension (Left) and curvatures (Right).

The time series is the first 468 seconds from a time series of three hours. The reason for picking such a short time series is that Bflex2010 has a limited memory, and thus an analysis of more than 5000 steps did not work with this model. In addition, some steps in the beginning of the analysis are used to apply tension and internal pressure. Based on the tension time series the tensions applied in the model to tune the results were the 300 kN, 350 kN and 400 kN, with the 350 kN used as an example in the following. These were bent well beyond full slip for two and a half cycles and results extracted. In addition to geometric information, the following need to be extracted from the results of the local analyses: The stress from axisymmetric loads at the given tension, σ_{tens}, the curvature are which slip occurs and the maximum corresponding friction stresses. The stresses at only axisymmetrical loads are found directly as the stresses in the tendons after the tension and inner pressure is applied, but before bending has commenced. Figure 5 show the tensions and the corresponding axial stresses in the tendons.

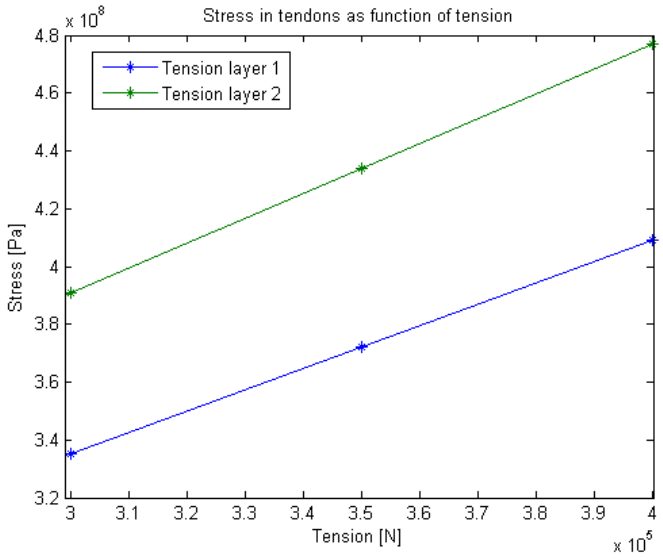

Figure 5: Direct computation: Stresses in tendons from axisymmetric loads.

As expected the stresses due to asymmetrical loads varies linearly with the tension applied. Figure 6 show the curvature and corresponding frictional stress in this model.

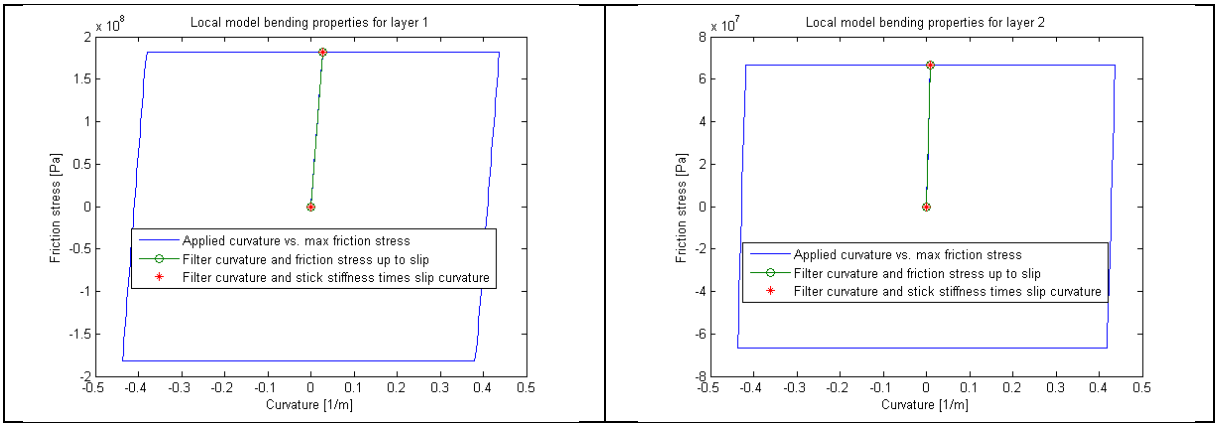

Figure 6: Direct computation; Curvature versus frictional stress for local model used for calibration. The tension is 350 kN.

As can be seen, due to the higher contact pressure, the maximum frictional stresses are much higher in the inner layer than the outer layer. Also in the figure, the stick stiffness is indicated along with the curvature and corresponding stress at which the stress transfer function goes from stick to slip. Figure 7 shows how slip curvature and stick stress changes with changing tension levels.

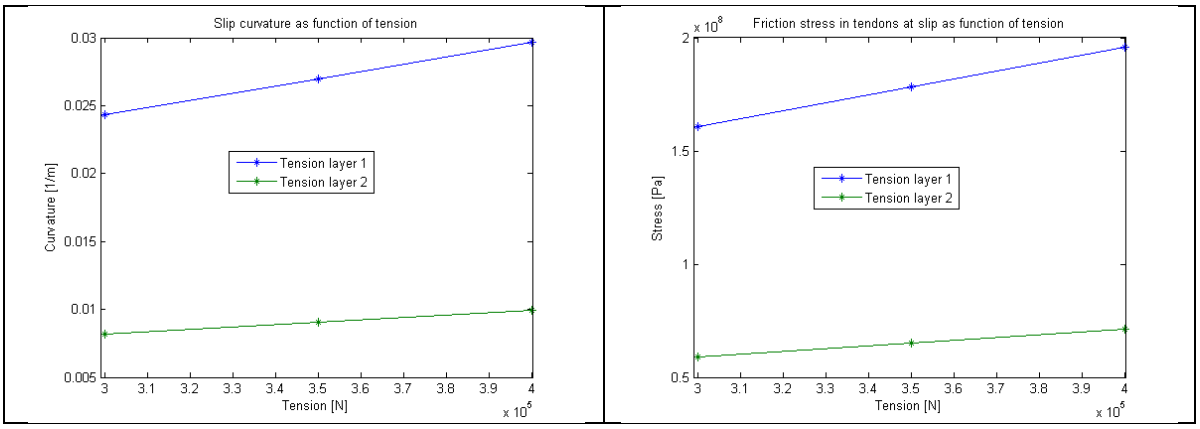

Figure 7: Direct computation: Slip curvature (Left) and friction stress at slip (Right) as function of tension.

Also here the relations are very close to linear.

Once calibrated with these values, the stress transfer function can be given the time series of tension and curvature. Stresses were calculated for both layers at the corners sixteen tendons around the cross section. The load at β equal to 45 degrees showed the largest tension variations. The stresses at βs equal to 0, 45 degrees 90 and 135 degrees of armor layer one will be emphasized in the following. Figure 8 show the stresses arising in tensile armor layer one from the tension variations.

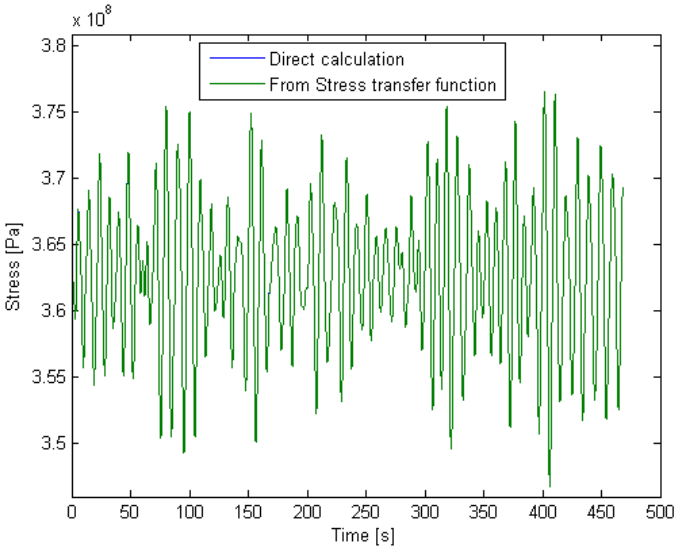

Figure 8: Stress from tension variations.

As the bending stresses showed very good agreement, only one sample is shown. Figure 9 shows the bending stresses for a β equal to 45 degrees, for the corner with positive local coordinates.

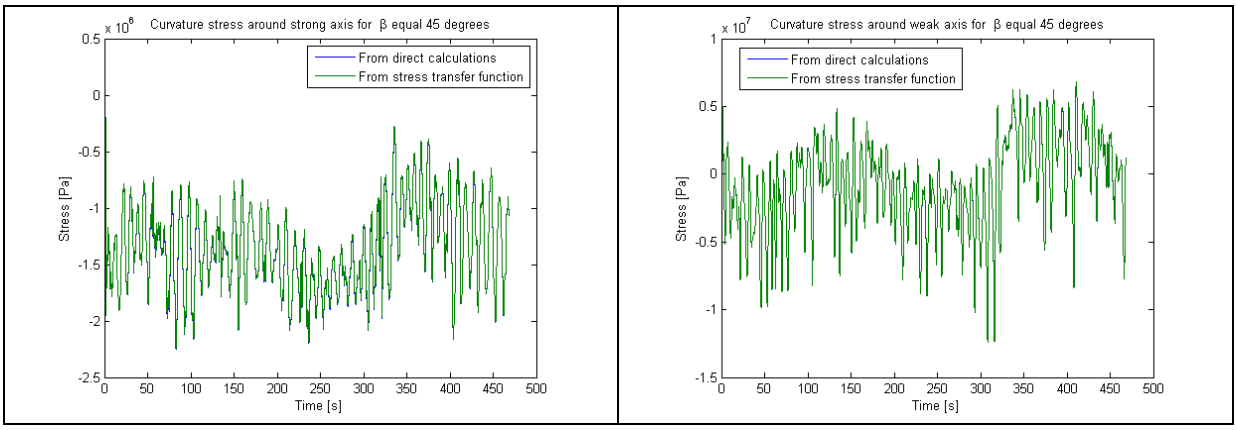

Figure 9: Bending around strong (Left) and weak (Right) axis of tendon at a β of 45 degrees.

As expected the bending stresses are close to identical for the two different methods. The stress variations due to bending are in the same magnitude range as the stresses from tension variations.

The last stress contribution is the frictional stresses. The global frictional stresses for the four different βs are shown in Figure 10.

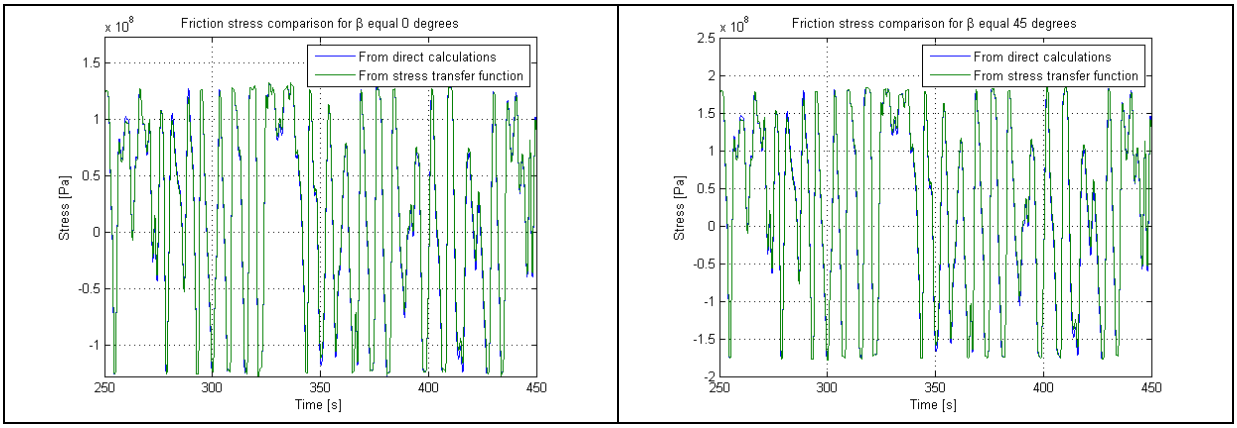

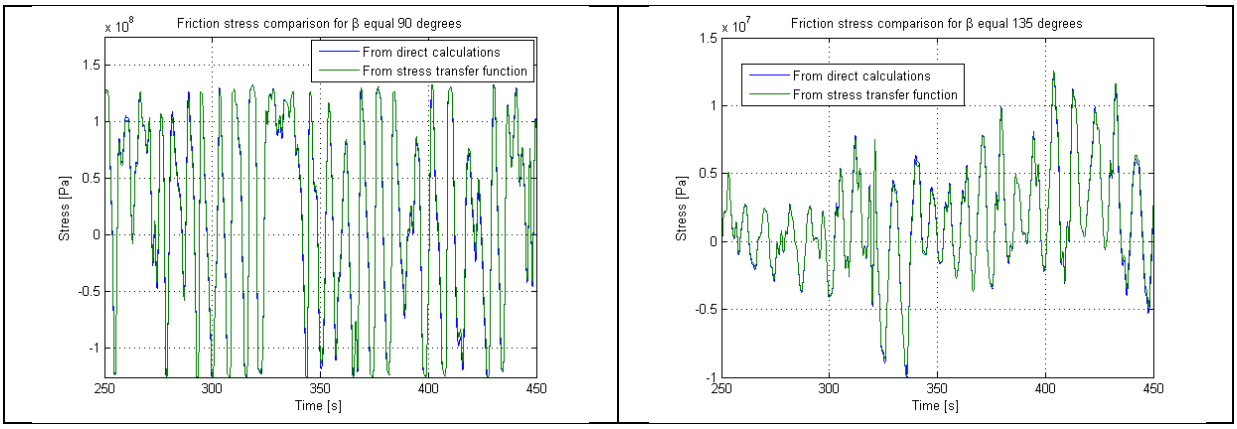

Figure 10: Comparison of frictional stresses for different βs from 250 to 450 seconds.

As can be seen, the results are nearly identical.

4 DISCUSSION

As can be seen from Figure 8 to Figure 10, the stress components are very close to identical. The stress from tension is a linear interpolation, by interval, of the stress at the input tensions of 300kN, 350kN and 400kN, and as the tensional stress is a linear function of tension (see Figure 5), this stress component should be mapped very closely. For the stresses due to bending of the tendons, the situation is similar. The equations to calculate the bending stresses are the same, and thus the bending stresses should be equal as well.

When it comes to the frictional stresses, the situation is a bit different. They are as mentioned history dependent, and small inaccuracies in the reading of the results from the local analysis may yield differences. However, as can be seen, the results are matching very well.

5 CONCLUSIONS

An implementation of a stress transfer function tuned with results from a local analysis is presented. The methodology, including assumptions has been explained, and a case study has been carried out. Both models are seen to have a conservative estimate on stress distribution around the cross-section.

As the curvatures from the global analysis are input to the stress transfer function, we do not need to do any equilibrium iterations. This leaves room for implementing more stick slip stations along the tendon as well as around the cross section in a computationally cheaper manner than in a finite element solver. Hence it may also be suitable as a testbed for hybrid analytical- numerical solutions taking multiaxiality and partial slip of the tendon into account.

ACKNOWLEDGEMENTS

This work has been partially supported by ANP (National Petroleum Agency) and by SINOCHEM do Brasil through the investment clause in Research, Development and Innovation. The authors would also like to acknowledge the support of CNPq through the program "RHAE Researcher in the Company" (561416-9/2010-9).

REFERENCES

API, 2009 Specification for Unbonded Flexible Pipe, *API 17J*, American Petroleum Institute

Doynov K. et al, 2007. Methodology for Calculating Irregular Wave Stress Time Histories of Tensile Wires in Flexible Risers, *OMAE2007-29104* proceedings

Sævik S., 1992. On stresses and fatigue in flexible pipes*, Ph.D. thesis*, NTH

Sævik S., 2010. Bflex2010 – Theory Manual*, Report number: MT70 F10-064*, MARINTEK, Trondheim.

Witz J.A.,1996. A Case Study in the Cross-section Analysis of Flexible Riser, *Marine Structures* 9, 885-904